

A lumped water balance model to evaluate duration and intensity of drought constraints in forest stands

A. Granier ^a, N. Bréda ^{a,*}, P. Biron ^b, S. Villette ^c

^a *Ecophysiologie Forestière, INRA, F-54 280 Champenoux, France*

^b *Centre d'Etudes et de Recherches Eco-Géographiques, CNRS, 3 rue de l'Argonne, F-67083 Strasbourg, France*

^c *Cycles Biogéochimiques, INRA, F-54 280 Champenoux, France*

Received 9 March 1998; accepted 30 October 1998

Abstract

This paper presents a daily water balance model where the main aim is to quantify drought intensity and duration in forest stands. This model requires daily potential evapotranspiration and rainfall as input climatic data. Required site and stand parameters are only maximum extractable soil water and leaf area index, the latter controlling (i) stand transpiration; (ii) forest floor evapotranspiration; and (iii) rainfall interception. Other informations, like root distribution and soil porosity, can be used if available, improving the simulation of short term soil water recharge. Water stress is assumed to occur when relative extractable soil water (REW) drops below a threshold of 0.4 under which transpiration is gradually reduced due to stomatal closure. The model was calibrated using sap flow measurements of stand transpiration in oak and spruce stands during several successive dehydration–rehydration cycles. Validation of the model was performed by comparing predicted soil water content to weekly neutron probe measurements in various forest stands and climatic conditions. The model simulated accurately the dynamics of soil water depletion and recharge, and predicted the main components of forest water balance. Day-to-day estimates of soil water content during the growing season allows to quantify duration and intensity of drought events, and to compute stress indexes. A dendroecological application is presented: a retrospective analysis of the effects of drought on radial tree growth, based on long term climatic time series, is shown. Some limitations and potential applications of the model are discussed. © 1999 Elsevier Science B.V. All rights reserved.

Keywords: Coniferous forest; Deciduous forest; Dendroecology; Drought; Forest; Leaf area index; Long term; Model; Transpiration; Water balance

* Corresponding author. Tel.: + 33-3-83394048; fax: + 33-3-83394022; e-mail: breda@nancy.inra.fr.

1. Introduction

The literature describes a wide variety of water balance models (mainly for agricultural and hydrological applications), that differ in their objectives, input data, complexity, spatial and temporal resolution. The main purpose of a water balance model is to predict temporal variations in soil water content, and to assess the water stress conditions actually experienced by a crop or a forest stand.

There is an increasing demand for large scale (region, continent) and for long term studies on forest–site–climate interactions, as much for hydrological as for forest management purposes. Such extensive applications require robust water balance models using simple soil and stand parameters and basic climatic data, in order to run simulations over many years. We developed a simple and lumped water balance model aimed basically at quantifying drought intensity and duration in forest stands. It uses a small set of parameters and standard daily meteorological data (potential evapotranspiration and precipitation). Evapotranspiration, which is generally the largest flux component, besides throughfall, is estimated here from ecophysiological relationships at stand scale. These relationships are driving by maximum leaf area index (LAI) to calculate canopy transpiration, understorey evapotranspiration and rainfall intercepted by tree canopies. It can be used for different sites and purposes, like long term (several years) or short term studies on the impact of drought on forest stands.

This model estimates the main terms of the hydrological cycle in forest stands: soil water content, stand transpiration and interception, drainage. It allows also to compute seasonal and annual integrated water stress indices to characterise drought events affecting physiological processes and growth of trees from various species, over long term periods.

This model was used for a retrospective analysis of the effects of drought on radial tree growth, and on crown conditions. It helped also to relate the effects of soil drought and tree physiology (Bréda, 1994), or nutrient dynamics in forest stands (Marques et al., 1996). It has

also been used for predictive applications, e.g. to simulate the consequences of various silvicultural management scenari (thinning intensity) or to quantify the consequences of global climate changes using data from the global climate model (GCM).

This paper describes the functions used in the model and its validation in various forest stands. Examples of annual variations in soil water content are shown for coniferous and broad-leaved stands growing on different soil types and under various climatic conditions. An example of long term analysis of the effects of water stress on radial growth of forest trees is also presented. Finally, a map of average water stress intensity in France is also shown.

2. List of symbols and abbreviations

Water fluxes and soil water content are expressed in mm H₂O that is 10⁻³ m³ per m² of ground area.

P	rainfall
Th	throughfall
In	rainfall interception
I_s	water stress index
T	tree transpiration
E_u	evaporation from understorey plus soil
PET	potential evapotranspiration (Penman formula)
ET	actual evapotranspiration = $T + E_u + In$
W	available soil water
W_m	minimum soil water (i.e. lower limit of water availability)
W_F	soil water content at field capacity
EW	extractable water = $W - W_m$
EW _M	maximum extractable water = $W_F - W_m$
REW	relative extractable water = $(W - W_m) / (W_F - W_m) = EW / EW_M$
REW _c	critical REW, at which tree transpiration begins to decrease
SWD	soil water deficit
D_i	drainage at the bottom of soil layer i
mic _{i}	microporosity of soil layer i
mac _{i}	macroporosity of soil layer i
f_i	water flow refilling soil layer i

3. Model description

This model is iterative and the variation in soil water content are calculated at a daily pace as:

$$\Delta W = P - I_n - T - E_u - D \quad (1)$$

where ΔW is the change in soil water content between two successive days.

3.1. Overstorey transpiration

Transpiration and rainfall interception are often modelled using mechanistic approaches derived from the Penman–Monteith equation (Monteith, 1973), which can be applied to the whole canopy as well as to a multi-layered vegetation. The Penman equation, which is defined on a 10-day, or a daily time basis, is considered as an index for evapotranspiration rather than a model, because it does not take into account surface resistance of the vegetation, and aerodynamic resistance is calculated using a unique relationship, independent of canopy structure. A comparison between the two approaches will be shown below. In the absence of significant difference in simulations of soil water content, we decided to use the Penman potential evapotranspiration equation, which is available in most national weather networks like Météo-France.

Work done at stand scale (but also at tree level, Levitt et al., 1995) showed a strong dependency of transpiration from potential evapotranspiration (PET) when soil water was not limiting. As reported for different species (Fig. 1) growing in various site conditions, under non-limiting soil water content and high LAI (≥ 6), the ratio $r = T/PET$ was 0.65–0.72 for *Pseudotsuga menziesii*, 0.75 for *Fagus sylvatica*, (Aussenac and Boulangeat (1980): water balance), 0.70–0.80 for *Quercus petraea*, (Bréda et al. (1993): sap flow and water balance), 0.70–0.80 for *Picea abies*, (Biron, 1994: sap flow and water balance). An average value of 0.75 for this ratio was used here. Below a LAI level of 6, an almost linear relationship was detected between r and LAI; this was true for comparison between different stands as well as for interannual variation in a given stand (Bréda and Granier, 1996).

We therefore used following relationship:

$$r = 0.125 * LAI \quad \text{if } 0 \leq LAI \leq 6.0$$

$$r = 0.75 \quad \text{if } LAI > 6.0 \quad (2)$$

Under water stress conditions, r was shown to decrease linearly (Fig. 2) as soon as REW decreased below a threshold (REW_c) of about 0.4, that is when soil water becomes limiting for transpiration. REW_c was found to be quite constant for several species, coniferous as well as broad-leaved, and whatever technique was used to estimate transpiration (Table 1). REW_c is basically a physiological threshold at which regulation of transpiration begins to occur due to stomatal closure. It was also shown to correspond to the cessation of radial increment (Fig. 3).

Coniferous species were assumed to keep a constant LAI and to transpire all over the year,

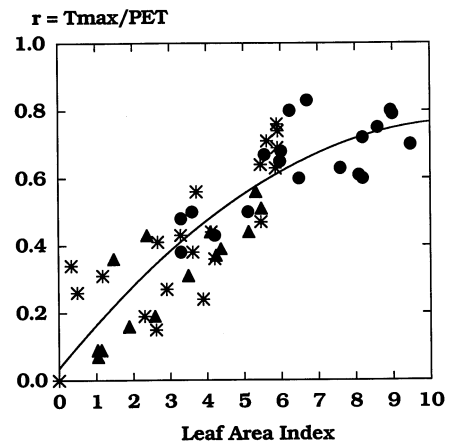


Fig. 1. Ratio (r) of stand transpiration (T_{\max}) to potential evapotranspiration (PET) under non-limiting soil water, as a function of stand leaf area index (LAI). Included data are: (1) intra-annual variations of LAI during spring leaf expansion (triangles) and autumn leaf fall (stars) are reported for an oak stand (data from Bréda, 1994), (2) inter-annual variations in maximum LAI (black circles) for an oak stand (data from Bréda and Granier, 1996) and reviewed from literature in different species and site conditions (*Fagus sylvatica* from Savoie et al., 1988 and Biron, 1994; mixed *Fagus* + *Quercus* from Aussenac and Granier, 1979; *Picea abies* from Cienciala et al., 1994 and Biron, 1994; *Pseudotsuga menziesii* from Black, 1979; Aussenac and Boulangeat, 1980; Granier, 1987; tropical rain forest from Granier et al., 1992, 1996; *Elaeis guineensis* from Dufrêne et al., 1992). Best fit is: $T_{\max}/PET = -0.006 * LAI^2 + 0.134 * LAI + 0.036$, $r^2 = 0.85$.

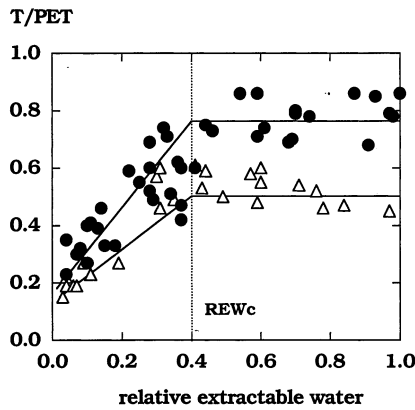


Fig. 2. Ratio T/PET calculated from sap flow measurements in an oak stand as a function of relative extractable water (REW) calculated from neutron probe measurements (from Bréda and Granier, 1996). Two data sets are reported: $LAI = 6 \text{ m}^2 \text{ m}^{-2}$ (black circles) and $LAI = 4.5 \text{ m}^2 \text{ m}^{-2}$ (open triangles). The dotted line shows the critical REW (REW_c).

including winter. In broad-leaved trees, $r = 0$ during the non-leaved period, and increases linearly at budbreak for 30 days, as measured on oaks by Bréda (1994). A symmetrical pattern was also assumed during leaf senescence and a linear decrease of r was assumed to occur for 30 days before leaf fall (Fig. 1).

3.2. Interception and throughfall

Modelling interception of precipitation from daily precipitation cannot be based on a mechanistic model like in Rutter et al. (1971), because it cumulates several rain events. Aussenac (Aussenac, 1968; Aussenac, 1972) showed a strong correlation between rainfall interception, incident

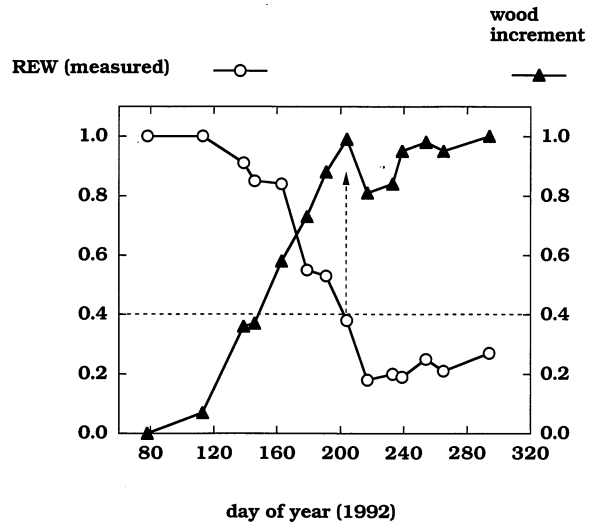


Fig. 3. Example of seasonal time course of the relative circumference increment (ratio of actual growth to maximum annual growth, triangles) of dominant oaks, as compared to the relative extractable water (REW, circles) calculated from neutron probe measurements. Dotted lines indicate circumference increment cessation and beginning of stem shrinkage, and the corresponding relative extractable water ($REW_c = \text{critical REW}$).

rainfall and light interception (R/R_0) in various coniferous and broadleaved stands, and different tree densities. A recent study performed in an oak stand by Bréda (1994) showed also a linear dependence of the relative rainfall interception to stand LAI in the range of 3 to $6 \text{ m}^2 \text{ m}^{-2}$. Rainfall interception is calculated in the model from functions proposed by Aussenac (1968):

$$In = P - \exp(a + b R/R_0 + cP + dP^2) \quad (3)$$

where

Table 1

Critical value of relative extractable water (REW_c) at which soil water content begins to limit maximum transpiration, i.e. to decrease the ratio $r = T/PET$

Reference	Species	REW_c	Method
Black, 1979	<i>Pseudostuga mensiezii</i>	0.4 (for both control and thinned)	Energy balance, Bowen ratio
Dunin and Aston, 1984	<i>Eucalyptus</i>	0.4	Lysimetry
Granier, 1987	<i>Pseudostuga mensiezii</i>	0.3	Sap flow
Biron, 1994	<i>Picea abies</i>	0.4	Sap flow, water balance
Bréda, 1994	<i>Quercus petraea</i>	0.4	Sap flow

$a = 0.186$, $b = 0.0027$, $c = 0.229$,

$d = -0.0043$ in broad-leaved stands,

$a = -0.124$, $b = 0.0080$, $c = 0.257$,

$d = -0.0058$ in coniferous stands.

Intercepted radiation R/R_0 is calculated from LAI using a standard value of extinction coefficient (see below).

In coniferous stands, this function is assumed to be constant all over the year. In broad-leaved stands, interception is reduced during the 30 days of leaf expansion and of leaf fall. If rainfall is less than 1 mm for broad-leaved and 2 mm for coniferous stands, interception is assumed to be 100% (Aussenac, 1975; Nizinski and Saugier, 1988).

As proposed by Rutter (1967), tree transpiration is reduced by 20% of the amount of intercepted water, because the rate of evaporation of intercepted water was shown to be on average approximately four times greater than transpiration rate.

Several authors (Stewart, 1977; Aussenac and Granier, 1979; Aussenac and Boulangeat, 1980) have shown that actual evapotranspiration could exceed PET due to the high rate of intercepted water evaporation. In our model, actual evapotranspiration was limited to 1.2 PET.

3.3. Understorey and soil evapotranspiration

Under many conditions, understorey and soil evapotranspiration cannot be neglected. Some experiments conducted in forests with a low LAI showed that E_u could reach 20–30% (Roberts et al., 1980; Granier et al., 1990) and sometimes up to 50% of ET (Kelliher et al., 1990). Recent studies have demonstrated that understorey vegetation was poorly coupled to the atmosphere (Jarvis and Mac Naughton, 1986; Berbigier et al., 1991; Kelliher et al., 1993). This means that understorey evapotranspiration is mainly depending upon net radiation reaching this level. Therefore, it was assumed that E_u (soil + understorey evapotranspiration) is proportional to the available energy reaching this level (see Diawara et al., 1991) when water is not limiting. Available energy below trees is proportional to global radiation

above the canopy, and dependent on LAI of the tree layer. In the model, available energy below the canopy is calculated from the Beer-Lambert function and a light coefficient of extinction (k). The literature reports a wide range of values for k , depending on stand structure, leaf area index and tree species. Jarvis and Leverentz (1983) proposed an average value of 0.5 for both coniferous and broadleaved species. In sessile oak stands, k varied between 0.4 and 0.5 (Bréda, 1994), for LAI between 2 and 5. Smith et al., (1991) and Pook (1984) proposed an estimated range of 0.4–0.6 for lodgepole pine and eucalyptus. In our model, we assumed an average value of 0.5.

Soil evaporation plus understorey transpiration were assumed to absorb water from the upper soil layer. In the absence of precise data on regulation of understorey transpiration during water stress, we assumed that it was linearly decreasing with relative extractable water in the upper soil layer.

3.4. Soil water content and drainage

According to the available information on soil characteristics and on rooting patterns, soil profiles can be described by an unique or by several horizontal layers. In each layer, water absorption by roots is assumed proportional to rooting density, as previously demonstrated in an intensive experiment of soil water dynamic and water uptake by roots (Bréda et al., 1995a,b). Total absorption from all the soil layers equals the sum of tree transpiration plus understorey evapotranspiration.

Throughfall water ($P - I_n$) vertically infiltrates in the soil. In each soil layer, the amount of water is divided into two components, their proportion depending on the distribution of pore sizes (Fig. 4): (1) water that quickly infiltrates through the macroporosity (gravitational water), reaching the following soil layer; (2) water stored in the microporosity which gradually refills the soil layer. When a layer i is rehydrated to field capacity, excess water D_i flows towards the consecutive layer by drainage. This procedure is more realistic

than that consisting to refill successively each layer to field capacity before to drain water in the following layer. Several field experiments have shown (unpublished data) that important drainage at the lower soil layers could occur in dry soils. The dynamic of field capacity recovery from dry conditions may therefore differ among soil layers, depending on pore size distribution, quantified by macro- and micro-porosity. If macro- and micro-porosity are not known, standard values may be used according to soil structure and texture.

Run-off is neglected, the model being used in areas covered by the vegetation on horizontal or gentle slopes.

3.5. Input data

Climatic variables are:

- daily PET, calculated from daily mean temperature ($^{\circ}\text{C}$), mean vapour pressure deficit (Pa), mean wind speed (m s^{-1}), daily cumulated global radiation (J m^{-2}) according to the recommendations of the European Community (Choisnel et al., 1992),
- daily cumulated rainfall (mm).

3.6. Parameters

The following stand and site parameters are necessary to run the model:

- maximum leaf area index (LAI);
 - maximum extractable water in the soil (EW_M). This value can be estimated either from soil texture in each horizon and using tables of equivalent water available per centimetre of soil (Hall et al., 1977) or from in situ water retention curves (Bréda et al., 1995a,b);
 - forest type: coniferous or broad-leaved; in broad-leaved stands the dates of beginning and end of the leafed period are required;
 - soil characteristics. In the absence of any further information, soil profile can be considered as only one layer including all the roots. More informations on the pedological characteristics of each horizon of the profile and rooting pattern improve the description of short term water dynamics in the soil, especially during rehydration.
- For each soil layer:
- percentage of fine roots,

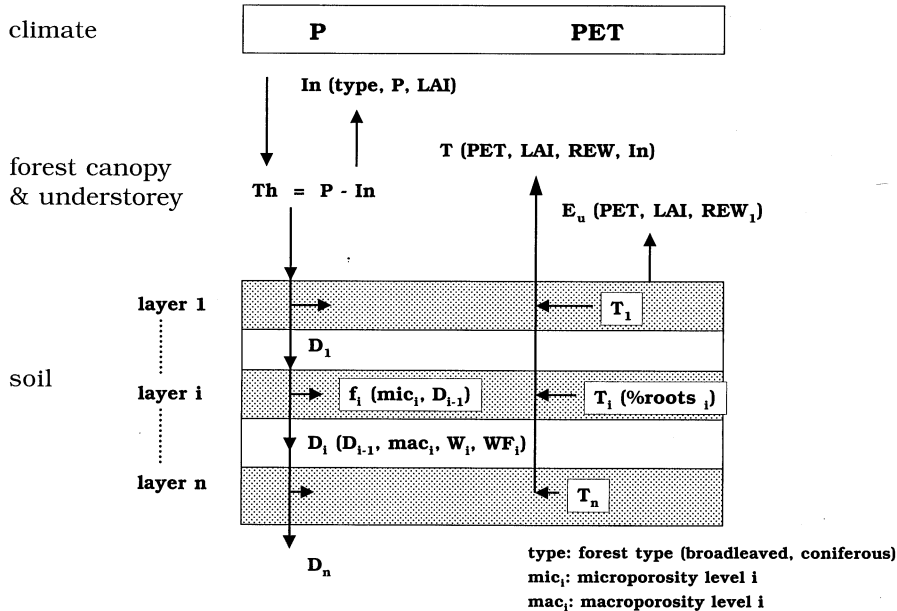


Fig. 4. Distribution of the two major water fluxes within and between the different soil layers: drainage (D) and water extraction by the root system (T). Symbols are defined in the text. D_n represents the drainage calculated at the bottom of the soil profile.

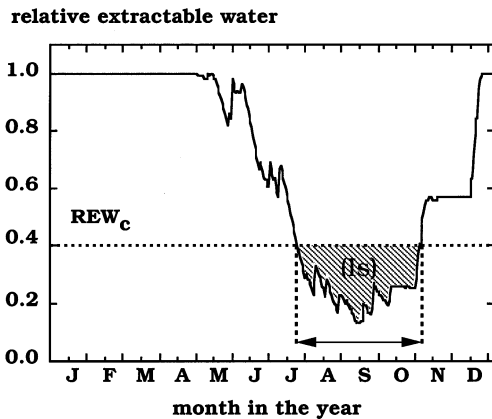


Fig. 5. Seasonal time course of relative extractable water (REW) in a soil, illustrating the number of days of water stress (segment with arrows) and the water stress index (I_s , dashed area). REW_c = critical REW.

- maximum extractable water EW_M ,
- macro- and micro-porosity.

3.7. Output variables

The different components of the water balance are computed daily: rainfall interception; throughfall; tree transpiration; understorey plus soil evaporation and drainage. Soil water content over the entire soil profile (W) and REW are calculated. Water stress is assumed to occur when REW drops below 40% of maximum extractable water; soil water deficit (SWD in millimetres) is therefore calculated daily against this threshold as:

$$SWD = (0.4 * EW_M - EW) \tag{4}$$

If $REW < REW_c$, two stress indexes are calculated, which can be monthly, seasonally or annually cumulated (Fig. 5):

- the number of days of water stress, i.e. the number of days during which $EW < 0.4 * EW_M$

- a water stress index (I_s , dimensionless), which cumulates the difference between REW and REW_c (corresponding to the dashed area in Fig. 5):

$$I_s = \sum SWD / EW_M \tag{5}$$

Finally, the links between the different functions described previously are illustrated in the flow chart presented in Fig. 6.

4. Comparison between hourly and daily models

We checked that: (i) the validity of using the Penman equation to estimate tree and overstorey transpiration; and (ii) the influence of hourly or daily time pace on the simulated soil water content. We compared the daily model to a hourly version which was based on the Penman–Monteith equation to estimate tree transpiration, and on equations of Rutter et al. (1971) for rainfall interception. The modelled variations of soil water content were tested with the two models over a 3-year period, using data from INRA-Champenoux weather station (near Nancy, France). Simulated values of REW calculated from both daily and hourly models are in good agreement (Fig. 7). A linear regression gives:

$$REW_{day} = 0.99 REW_{hour} + 0.03 \quad r^2 = 0.98$$

For long term studies, a daily pace of modelling can therefore be considered to present a sufficient accuracy.

5. Validation

Validation of the model was done by comparing simulated and measured soil water, using

Fig. 6. Flow chart of the water balance model. The model is iterative and the presented loop is run day after day. The successive steps are: (1) LAI defines understorey evapotranspiration (1–1), rainfall interception (1–2) and overstorey transpiration (1–3); (2) throughfall is calculated according to forest type, LAI and incident rainfall; (3) throughfall is added to the available soil water of the previous day $n - 1$. The new available soil water is calculated and compared to maximum soil water to define drainage (5) or soil water deficit (6). If soil water deficit occurs (7) or if the canopy is wet (8), the r ratio is reduced. Overstorey transpiration (9) and understorey evapotranspiration (10) are then subtracted to soil water content. Daily water fluxes and drought indices are finally computed (11).

Daily climatic inputs :
precipitation, PET (global radiation, wind speed,
temperature, vapour pressure deficit)

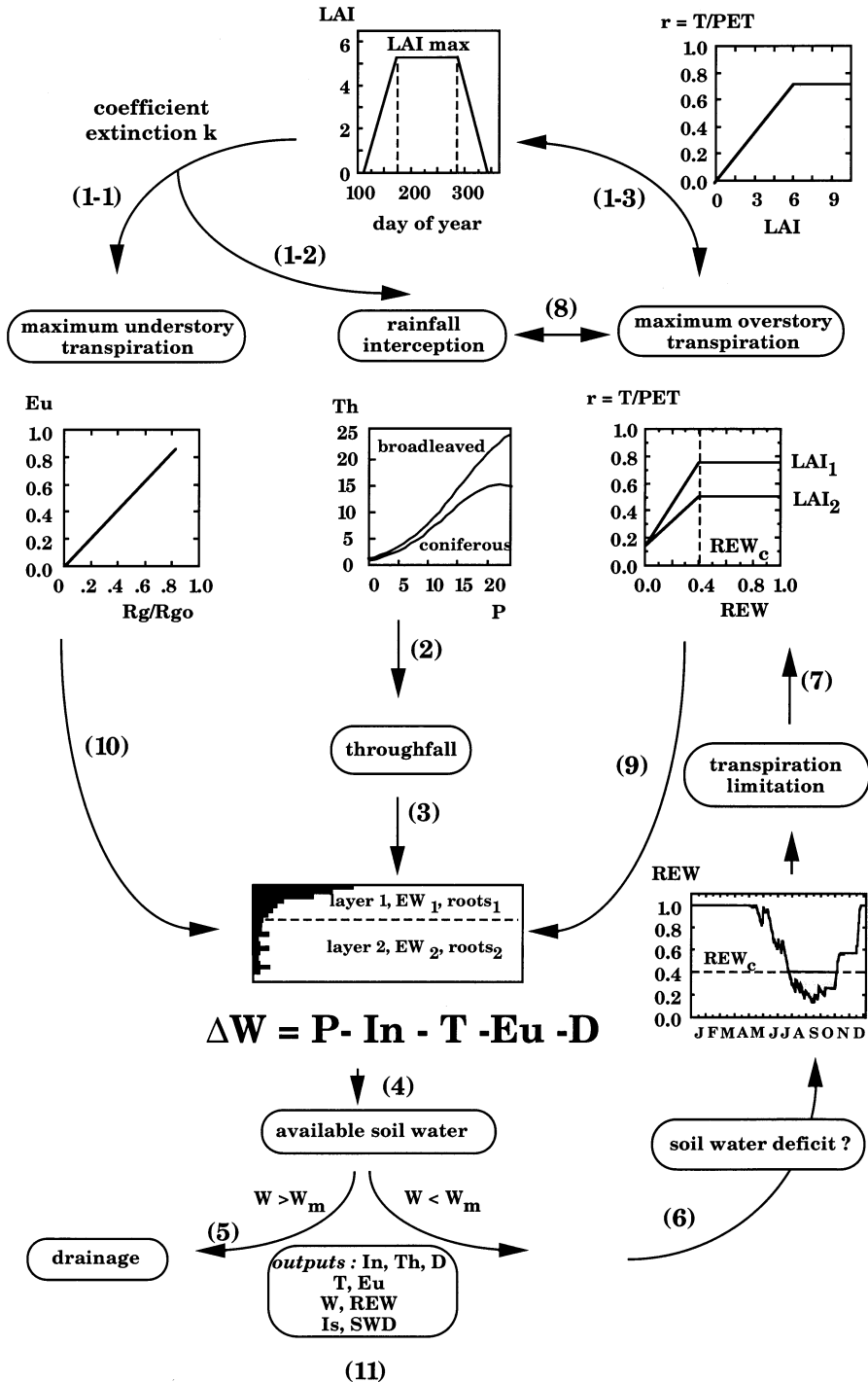


Fig. 6.

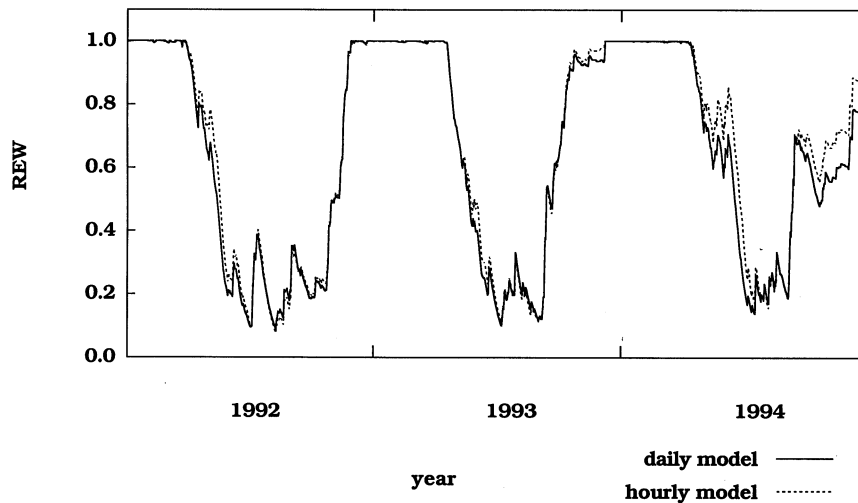


Fig. 7. Time-course of relative extractable water (REW) simulated with the daily water balance model using Penman potential evapotranspiration (full line) as compared to REW estimated from a hourly model using Penman–Monteith (dotted line).

weekly measurements with a neutron probe in various forest stands differing in structure, species composition, climate and soil conditions.

The first stand was a 30-year-old oak (*Quercus petraea*) plain forest, which was extensively described by Bréda et al. (1993). A second stand was a 30-year-old spruce (*Picea abies*) forest (Biron, 1994) located in the Vosges mountain, at 1000 m elevation. In both stands, measurements were performed during three successive years and a good agreement between modelled vs. measured REW is observed in both stands (Fig. 8).

Other validations were performed in a natural beech forest and in a Douglas-fir plantation described by Aussenac and Granier (1979) and Aussenac and Granier (1988), respectively. Fig. 9 shows the comparison of measured versus simulated REW, for 1 year in the beech stand, and for 3 years in the Douglas-fir stand. Agreement was good in both stands, even if a slight time lag can be observed during the beginning of the summer when soil water content decreased, probably due to a difference between actual budburst dates and the unique value taken to run the model.

6. Examples of seasonal pattern of REW

Three simulations of the time course of REW during 4 contrasted years are shown in Fig. 10. The first one corresponds to a coniferous stand growing on a deep soil ($EW_M = 180$ mm), the two others to broad-leaved stands growing on a deep ($EW_M = 185$ mm), and on a shallow ($EW_M = 72$ mm) soil, respectively. Due to differences in phenology, water reserve under the coniferous was depleted earlier during spring and early summer, while full recovery of field capacity during autumn occurred at the same time for broad-leaved and coniferous forests, due to heavy autumn rainfall every year.

The largest difference between soil with high and low extractable water can be observed during the wettest years. Critical REW was reached earlier in the season in the shallower soils, and REW remained above the threshold in deeper soils. Short term variations of REW were also larger in superficial soil conditions. On the contrary, little differences between stands appeared during the driest year (1991): soil water reserve was completely depleted, and REW reached zero on both stands. Water stress indexes (number of

days of WS and I_s values) were very close during this year. During dry years, water depletion during spring occurred earlier, and water recharge was earlier in autumn in the most superficial soil.

7. Example of use of water stress index

In a regional dendroclimatological study (Badeau, 1995), inter-annual variations of radial growth in plain stands of beech (*Fagus sylvatica*) were analysed in relation to climate. Water balance simulation was made on a 42 year (1950–1991) climatic time-series in order to calculate the seasonal stress index (I_s) (from budburst to the end of August). The influence of water deficits on tree growth has to be analysed without confusing factors, especially the effect of age has to be removed from the individual radial growth of trees. This was achieved by: (1) calculating a reference growth

- spruce stand
 $REW_p = 0.99 * REW_o + 0.03 \quad r^2 = 0.75$
- ▲ oak stand
 $REW_p = 1.09 * REW_o - 0.08 \quad r^2 = 0.90$

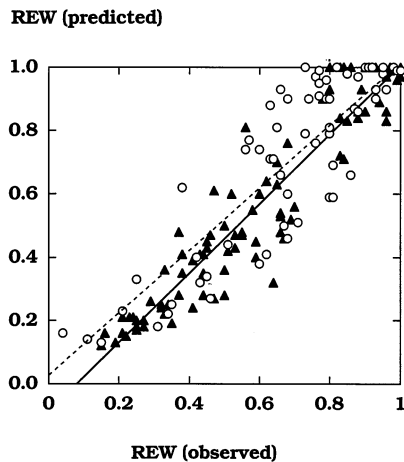


Fig. 8. Validation of the water balance model: comparison of the seasonal time course of relative extractable water (REW) measured with neutron probe and REW predicted by the model. Data from an oak stand in Champenoux Forest (black triangles, Bréda, 1994, LAI = 6, $EW_M = 180$ mm) and from a spruce stand in Aubure Forest (open circles, Biron, 1994, LAI = 8, $EW_M = 100$ mm). The r^2 coefficients are 0.90 and 0.75, respectively.

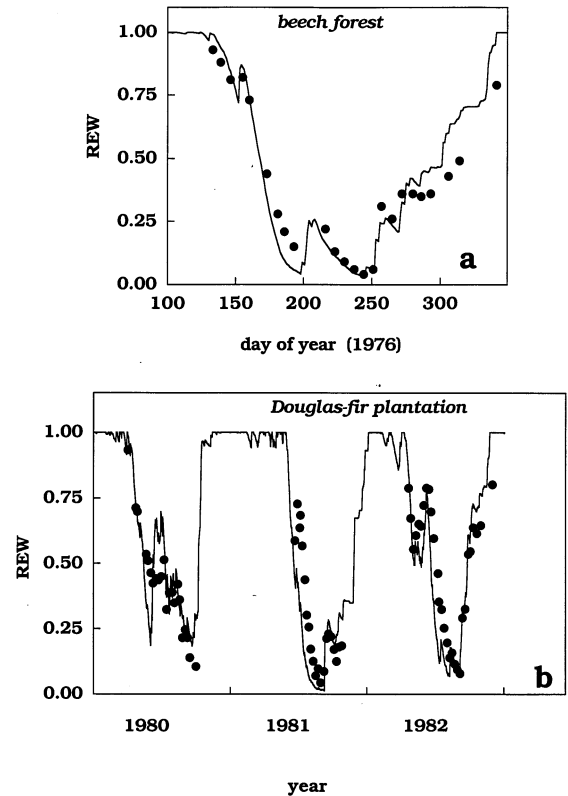


Fig. 9. Validation of the water balance model: comparison of measured and simulated REW in two forest stands. (a) natural beech stand ($LAI = 6.2 \text{ m}^2 \text{ m}^{-2}$, $EW_M = 150$ mm); (b) Douglas-fir plantation ($LAI = 7.0 \text{ m}^2 \text{ m}^{-2}$, $EW_M = 130$ mm). Dots: measured; lines: simulated.

curve according to tree age on a large sample of trees; and (2) calculating the radial growth index, ratio of each actual ring width versus the reference radial growth. Radial growth index of year n was then related to water stress indexes $I_s(n)$ and to $I_s(n-1)$ of years n and $n-1$, in order to take into account the present and the after-effects of water stress. A linear regression with two variables showed a high correlation ($r^2 = 0.65$, Fig. 11).

8. Example of drought diagnosis at a regional scale

Analysis of spatial and temporal variation in soil water availability and prediction of regional drought risks are of major interest for forest

management. To characterise annual (average) local water stress conditions in forests or quantification of exceptional droughts, relevant variables are the mean drought duration and the maximal drought intensity. As an example, the model was run for a ‘standard’ broad-leaved stand, growing on a soil with an extractable water of 140 mm in different regions of France. Climatic data were obtained from 12 weather stations (Météo-France network) close to large forested areas, over an 11 year period (1983–1993); this time period is statistically long enough to take into account inter-annual variability of the climate (Choisnel, 1992). Fig. 12 shows spatial distribution of the average number of days of water stress over the 11 years. Average annual water stress duration lasted more than 1 month in all sites with the exception of one site (Pau), while maximum drought duration in the driest site (Colmar) lasted over 2.5 months.

9. Discussion

The main advantage of the model presented here is that it uses in its basic version only two parameters, leaf area index and maximum extractable water in the soil, which can be easily measured or

estimated. Maximum extractable water can be calculated from simple field measurements (depth, texture, porosity). This allows simulations to be performed over a wide range of soil types and tree species.

To simulate water transfer in the soil, we decided not to use hydraulic parameters like hydraulic conductivity, which are difficult to measure and which show a high spatial variability (Wopereis et al., 1993, Leenhardt et al., 1994). The model simulates quite well the short term water dynamics in the soil, as we observed by comparing simulated to measured soil water content profiles using the neutron probe technique (data not shown), during drought development or rewatering. The main advantage of our approach is to allow a more or less detailed parametrization, depending on the available soil characteristics. We tested also the sensitivity of the model to soil parametrization by comparing simulations using a default set of parameters (according to the soil texture) to simulations using in situ observations of rooting pattern, soil porosity and density in each layer. We concluded that a standard set of parameters did not modify water stress indexes to a large extent, but only lead to a time lag in soil reserve increase during the period when soil is refilling in autumn.

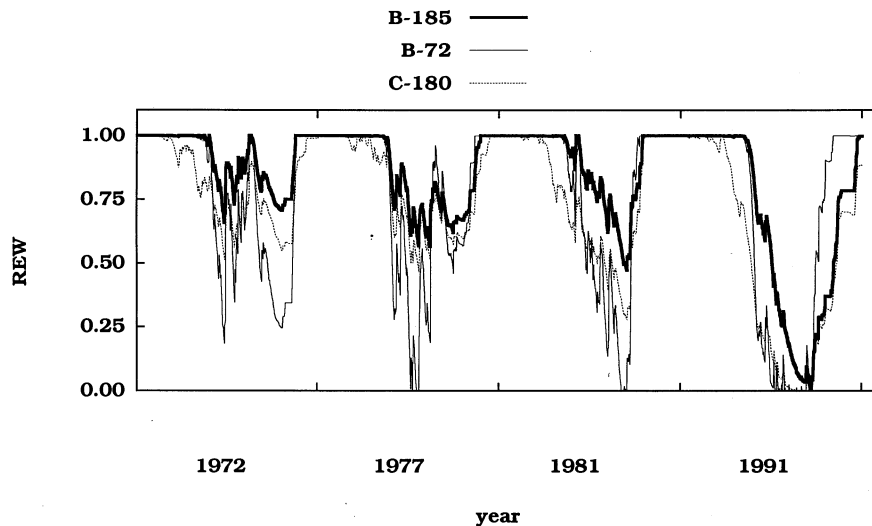


Fig. 10. Simulation of time course of relative extractable water in the soil (REW) during 4 years with contrasted climate patterns. Simulations were run for a broad-leaved stand (beech) with two different levels of extractable soil water (B-185 mm and B-72 mm) and for a coniferous (Douglas-fir) stand (C-180 mm); weather input data are from Nancy (Météo-France).

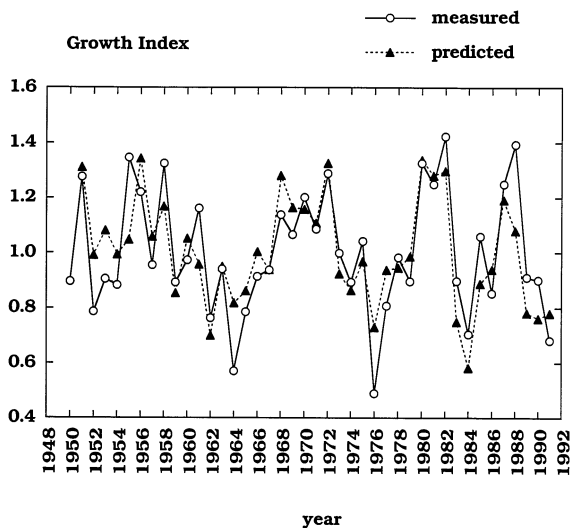


Fig. 11. Inter-annual variations of radial growth index of *Fagus sylvatica* as measured on cores (Badeau, 1995) compared to predicted growth index. Predicted growth index was calculated from a linear model with two variables taking into account simulated soil water deficit (L_s), cumulated from budburst to the end of August, for the current and for the previous years. See comments in the text.

The model uses constant dates of budburst and leaf fall and no climate-dependent function of phenological development is yet included in the model. In order to analyse the sensitivity to phenology, simulations have been run in oak over years when budburst and leaf fall dates were observed (Bréda, 1994). We showed that stress indexes were not significantly changed by budburst. This is due to several reasons: (1) the interannual variability in budburst and leaf fall dates is low (max. 10 days) under 'normal' conditions; (2) during spring, the soil reservoir is full filled while evaporative demand is quite low under temperate climate. Water consumption during leaf expansion or leaf fall represents less than 5% of seasonal water uptake on oaks (Bréda, unpublished data). Nevertheless, when budburst is largely delayed due to accidents (e.g. spring frost, caterpillars), discrepancies between measured and simulated soil water content can be observed, and actual phenological data are required in this case.

Maximum LAI has been shown to be one of the most important parameters, because stand

transpiration, rainfall interception and understorey evapotranspiration are directly depending on it. We therefore would need further information about the determination of inter-annual variation of LAI (according to stand age and climatic conditions of current and previous years).

The model was calibrated and validated in closed stands, and several improvements are necessary to extend simulations to open stand conditions and to thinned stands. In open stands, the contribution of understorey to total evapotranspiration can be quantitatively important and participates to soil water deficit in a large extent (Roberts et al., 1980; Petersen et al., 1988; Granier et al., 1990). The simplest approach is to relate available energy below the canopy to stand LAI, and hence to potential transpiration of the understorey. But information on stomatal control of water loss, its relationship with soil water depletion and phenological development, is still missing for many species (for both herbaceous and coppice) growing in the understorey. The effect of thinning on water balance has been quantified in some coniferous (Black, 1979; Donner and Running, 1986; Aussenac and Granier, 1988; Stogsdill et al., 1992) and in a few broad-leaved stands (oaks, Bréda et al., 1995a; Bréda et al., 1995b). Both stand transpiration and rainfall interception are generally higher in thinned than in control stands at a given LAI several years after thinning. It is however still not clear how long it takes for the stand to recover a new equilibrium, corresponding to canopy closure. In a young Douglas-Fir stand (Aussenac and Granier, 1988), canopy closure was recovered within 5 years. But the duration of this unbalanced period following thinning may probably vary according to factors influencing the dynamics of canopy and root expansion (tree species, age, thinning intensity, etc.).

Due to the robustness of the model and its easy parametrisation for a large range of species and soil types, many ecological applications can be considered on both inter- and intra-annual basis. First, long climatic time series can be used for simulations in the frame of forest survey projects. Water stress indexes are already used in the analysis of inter-annual radial growth (Fig. 11), and

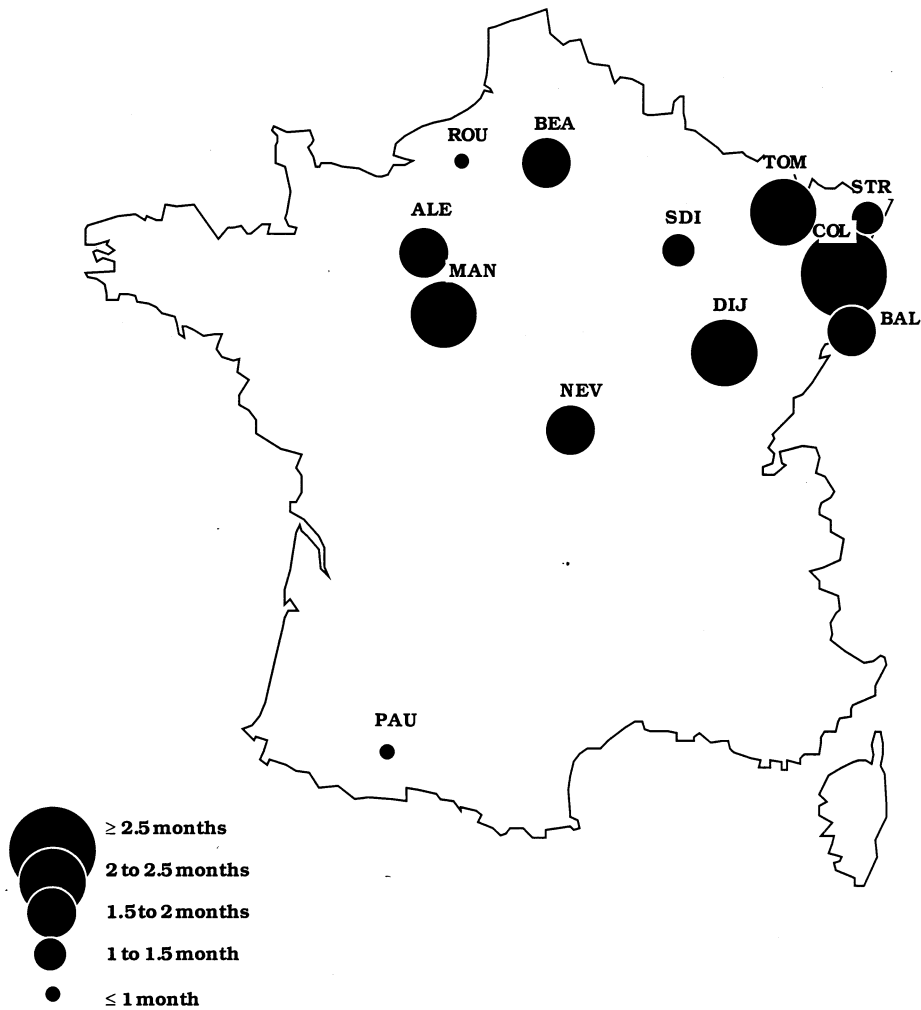


Fig. 12. Mean annual water stress duration, calculated for 12 weather stations in France (data Météo-France), as the number of days of water deficit averaged over the 1983–1993 period. Size of the symbols is proportional to drought duration, represented by 15 days categories, the smallest symbol representing 1 month and the largest one over 2.5 months.

also of temporal and spatial variations in crown conditions, observed through crown transparency in forest survey networks. Some applications in a predictive way are also being tested, like quantification of the effects of global change on water stress in forest.

More generally, simulations of soil water content and drought assessment are useful tools for separating climate from other effects (biotic, fertilisation, silvicultural practices, etc.) in ecological projects. Finally, the combination of pedological data base and climatic network

allow to simulate quite in real time forest water balance and to draw forest water stress maps, as already done for crops (Choisnel and Jacquart, 1991). This could be of major interest for forest health and productivity programmes.

References

- Aussenac, G., 1968. Interception des précipitations par le couvert forestier. *Ann. Sci. For.* 25, 135–156.

- Aussenac, G., 1972. Etude de l'évapotranspiration réelle de quatre peuplements forestiers de l'est de la France. Ann. Sci. For. 29, 369–389.
- Aussenac, G., 1975. Couverts forestiers et facteurs du climat: leurs interactions, conséquences écophysologiques chez quelques résineux. Thèse Université de Nancy I, 227 pp.
- Aussenac, G., Boulangeat, C., 1980. Interception des précipitations et évapotranspiration réelle dans des peuplements de feuillu (*Fagus sylvatica* L.) et de résineux (*Pseudotsuga menziesii* (Mirb. Franco). Ann. Sci. For. 37, 91–107.
- Aussenac, G., Granier, A., 1979. Etude bioclimatique d'une futaie feuillue (*Fagus sylvatica* et *Quercus sessiliflora* Salisb.) de l'Est de la France. II. Etude de l'humidité du sol et de l'évapotranspiration réelle. Ann. Sci. For. 36, 265–280.
- Aussenac, G., Granier, A., 1988. Effects of thinning on water stress and growth in douglas fir. Can. J. For. Res. 18, 100–105.
- Badeau, V., 1995. Etude dendroécologique du hêtre (*Fagus sylvatica* L.) sur les plateaux calcaires de Lorraine. Thèse Université Nancy I, 224 pp.
- Berbigier, P., Diawara, A., Loustau, D., 1991. A microclimatic study of the effect of drought on evapotranspiration in a maritime pine stand and its understorey. Ann. Sci. For. 48, 157–177.
- Biron, P., 1994. Le cycle de l'eau en forêt de moyenne montagne: flux de sève et bilans hydriques stationnels (bassin versant du Strengbach à Aubure-Hautes Vosges). Thèse de l'Université Louis Pasteur (Strasbourg), 244 pp. + annexes.
- Black, T.A., 1979. Evapotranspiration from Douglas fir stands exposed to soil water deficits. Water Resour. Res. 15, 164–170.
- Bréda, N., 1994. Analyse du fonctionnement hydrique des chêne sessile (*Quercus petraea* (Matt.) Lieb) et pédonculé (*Quercus robur* L.) en conditions naturelles; effets des facteurs du milieu et de l'éclaircie. Thèse Université Nancy I, 50 pp. + publications.
- Bréda, N., Cochard, H., Dreyer, E., Granier, A., 1993. Seasonal evolution of water transfer in a mature oak stand (*Quercus petraea* Matt. Liebl.) submitted to drought. Can. J. For. Res. 23, 1136–1143.
- Bréda, N., Granier, A., 1996. Intra- and inter-annual variations of transpiration, leaf area index and radial growth of a sessile oak stand (*Quercus petraea*). Ann. Sci. For. 53, 521–536.
- Bréda, N., Granier, A., Barataud, F., Moyne, C., 1995a. Soil water dynamics in an oak stand. Part I. Soil moisture, water potentials and root water uptake. Plant Soil 172, 17–27.
- Bréda, N., Granier, A., Aussenac, G., 1995b. Effects of thinning on soil and tree water relations, transpiration and growth in an oak forest (*Quercus petraea* (Matt.) Liebl.). Tree Physiol. 15, 295–306.
- Choisnel, E., 1992. L'analyse spatiale du bilan hydrique en agrométéorologie. La Météorologie 43–44, 31–42.
- Choisnel, E., de Villèle, O., Lacroze, F., 1992. Une approche uniformisée du calcul de l'évapotranspiration potentielle pour l'ensemble des pays de la Communauté Européenne. Centre Commun de Recherche, Commission des Communautés Européennes, EUR 14223, 177 pp.
- Choisnel, E., Jacquart, C., 1991. Les sécheresses et leurs diagnostics: qualité et rapidité d'information. C.R. Acad. Agri. Fr. 77, 65–74.
- Cienciala, E., Eckersten, H., Lindroth, A., Hallgren, J.E., 1994. Simulated and measured water uptake by *Picea abies* under non limiting soil water conditions. Agric. For. Meteorol. 71, 147–164.
- Diawara, A., Loustau, D., Berbigier, P., 1991. Comparison of two methods for estimating the evaporation of a *Pinus pinaster* (Ait.) stand: sap flow and energy balance with sensible heat flux measurements by an eddy covariance method. Agric. For. Meteorol. 54, 49–66.
- Donner, B.L., Running, S.W., 1986. Water stress response after thinning *Pinus contorta* stands in Montana. For. Sci. 32, 614–625.
- Dufrène, E., Dubos, B., Rey, H., Quencez, P., Saugier, B., 1992. Changes in evapotranspiration from an oil palm stand (*Elaeis guineensis* Jacq.) exposed to seasonal soil water deficits. Acta Ecol. 13, 299–314.
- Dunin, F.X., Aston, A.R., 1984. The development and proving of models of large scale evapotranspiration: an Australian study. In: Sharma, M.L. (Ed.), Evapotranspiration from Plant Communities. Elsevier, Amsterdam, pp. 305–323.
- Granier, A., 1987. Evaluation of transpiration in a Douglas-fir stand by means of sap flow measurements. Tree Physiol. 3, 309–320.
- Granier, A., Bobay, V., Gash, J.H.C., Gelpe, J., Saugier, B., Shuttleworth, W.J., 1990. Vapour flux density and transpiration rate comparisons in a stand of Maritime Pine (*Pinus pinaster* Ait.) in Les Landes forest. Agric. For. Meteorol. 51, 309–319.
- Granier, A., Huc, R., Barigah, S.T., 1996. Transpiration of natural rain forest and its dependence on climatic factors. Agric. For. Meteorol. 78, 19–29.
- Granier, A., Huc, R., Colin, F., 1992. Transpiration and stomatal conductance of two rain forest species growing in plantations (*Simarouba amara* and *Goupia glabra*) in French Guyana. Ann. Sci. For. 49, 17–24.
- Hall, D.G.M., Reeve, M.J., Thomasson, A.J., Wright, V.F., 1977. Water retention, porosity and density of field soils. Soil survey of England and Wales, Technical monograph no. 9. Harpenden. 75 pp.
- Jarvis, P.G., Leverenz, J.W., 1983. Productivity of temperate, deciduous and evergreen forests. In: Lange, O.L., et al. (Eds.), Physiological Plant Ecology IV, Encyclopedia of Plant Physiology, vol. 12D. Springer, Berlin.
- Jarvis, P.G., Mac Naughton, K.G., 1986. Stomatal control of transpiration: Scaling up from leaf to region. In: Kozlowski, K. (Ed.), Advances in Ecological Research, vol. 15. Academic Press, London, pp. 1–49.
- Kelliher, F.M., Whitehead, D., McAneney, K.J., Judd, M.J., 1990. Partitioning evapotranspiration into tree and understorey components in two young *Pinus radiata* D. Don stands. Agric. For. Meteorol. 50, 211–227.

- Kelliher, F.M., Leuning, R., Schulze, E.D., 1993. Evaporation and canopy characteristics of coniferous forests and grasslands Review. *Oecologia* 95, 153–163.
- Leenhardt, D., Voltz, M., Bornand, M., 1994. Propagation of the error of spatial prediction of soil properties in simulating crop evapotranspiration. *Eur. J. Soil Sci.* 45, 303–310.
- Levitt, D.G., Simpson, J.R., Tipton, J.L., 1995. Water use of two landscape tree species in Tucson, Arizona. *J. Am. Soc. Hortic. Sci.* 120, 409–416.
- Marques, R., Ranger, J., Villette, S., Granier, A., 1996. Nutrient dynamics in a chronosequence of Douglas-fir (*Pseudotsuga menziesii* (Mirb.) Franco) stands on the Beaujolais Mounts (France). 2 Quantitative approach. *For. Ecol. Manage.* 92, 167–197.
- Monteith, J.L., 1973. *Principles of Environmental Physics*. Edward Arnold, London.
- Nizinski, J., Saugier, B., 1988. Mesures et modélisation de l'interception nette dans une futaie de chênes. *Ecol. Plant.* 9, 311–329.
- Petersen, T.D., Newton, M., Zedaker, S.M., 1988. Influence of *Ceanothus velutinus* and associated forbs on the water stress and stemwood production of Douglas-fir. *For. Sci.* 34, 333–343.
- Pook, E.W., 1984. Canopy dynamics of *Eucalyptus maculata* Hook. II. Canopy leaf area balance. *Aust. J. Bot.* 32, 405–413.
- Roberts, J., Pymar, C.F., Wallace, J.S., Pitman, R.M., 1980. Seasonal changes in leaf area, stomatal and canopy conductances and transpiration from bracken below a forest canopy. *J. Appl. Ecol.* 17, 409–422.
- Rutter, A.J., 1967. An analysis of evaporation from a stand of Scots pine. In: Sopper, W.E., Lull, H.W. (Eds.), *Forest Hydrology*. Pergamon Press, Oxford.
- Rutter, A.J., Kershaw, K.A., Robin, P.C., Morton, A.J., 1971. A predictive model of rainfall interception in forests. I. Derivation of the model from observations in a plantation of Corsican pine. *Agric. Meteorol.* 9, 367–384.
- Savoie, J.M., Comps, B., Letouzey, J., Gelpe, J., 1988. Bilan hydrique des hêtraies mixtes en relation avec le comportement et la régénération du Hêtre (*Fagus sylvatica* L.). *Ecol. Plant.* 9, 285–300.
- Smith, F.W., Sampson, D.A., Long, J.N., 1991. Comparison of leaf area estimates from tree allometrics and measured light interception. *For. Sci.* 37, 1682–1688.
- Stewart, J.B., 1977. Evaporation from the wet canopy of a pine forest. *Water Resour. Res.* 13, 915–921.
- Stogsdill, W.R., Wittwer, R.F., Hennessey, T.C., Dougherty, P.M., 1992. Water use in thinned loblolly pine plantations. *For. Ecol. Manage.* 50, 233–245.
- Wopereis, M.C.S., Kropff, M.J., Wosten, J.H.M., Bouma, J., 1993. Sampling strategies for measurement of soil hydraulic properties to predict rice yield using simulation models. *Geoderma* 59, 1–20.